Generation of entanglement density within a reservoir

C Lazarou, B M Garraway, J Piilo, S Maniscalco

Generation of entanglement density within a reservoir

C. Lazarou

Department of Physics and Astronomy, University College London, Gower Street, London WC1E 6BT, United Kingdom
Department of Physics, Sofia University, James Bourchier 5 Boulevard, 1164 Sofia, Bulgaria

B. M. Garraway

Department of Physics and Astronomy, University of Sussex, Falmer, Brighton, BN1 9QH United Kingdom

J. Piilo

Turku Centre for Quantum Physics, Department of Physics and Astronomy, University of Turku, FI-20014 Turun yliopisto, Finland

S. Maniscalco

Turku Centre for Quantum Physics, Department of Physics and Astronomy, University of Turku, FI-20014 Turun yliopisto, Finland

Abstract. We study a single two-level atom interacting with a reservoir of modes defined by its reservoir structure function. Within this framework we are able to define a density of entanglement involving a continuum of reservoir modes. The density of entanglement is derived for a system with a single excitation by taking a limit of the global entanglement. Utilizing the density of entanglement we quantify the entanglement between the atom and the modes, and also between the reservoir modes themselves.

PACS numbers: 03.67.Mn, 03.65.Yz, 03.67.Bg

Submitted to: *New J. Phys.*

1. Introduction

In recent years, entanglement has attracted the attention of many physicists working in the area of quantum mechanics [1, 2]. This is due to the ongoing research in the area of quantum information [3], and also because of the advances made in different experimental disciplines, such as in ion traps [4] and Bose-Einstein condensation [5, 6]. Developments in the field of cavity QED, where experiments in the strong coupling regime are carried out [7,8] provide plenty of motivation for studying quantum information and entanglement. Theoretical studies are also important in the context of atom-light interactions inside structured reservoirs [9] such as resonant cavities or photonic band gap materials. The theoretically predicted atom-photon bound state could also lead to entanglement and this can also be linked to another problem: that of atom-laser out-coupling from Bose-Einstein condensates [10–12], where analogous effects were predicted in the past.

Besides entangling atoms with each other, or atoms with a few modes, or modes with each other, it is clear that even a single atom can become entangled with a *reservoir* comprised of modes. The issue we address here is how to describe this kind of entanglement. In the analysis of Ref. [13] the reservoir is treated (in a limiting process) as a collective object, and the entanglement between the atom and each reservoir mode, or between the modes, is not considered. It is also possible to partition the reservoir [14] and then study entanglement between these partitions using a Weisskopf-Wigner theory for a decaying two-level atom.

In the present work we study entanglement between the atom and the reservoir by means of an *entanglement density* which can apply to non-Markovian systems, too. In our model, an atom interacts with a continuum of modes at zero temperature [15, 16], and entanglement properties between the atom and the modes and also between the modes are considered. Using global entanglement as a measure of entanglement, we derive a pair of distributions that can be interpreted as *densities of entanglement* in terms of all the reservoir modes. Both distributions can be calculated in terms of the spectrum of reservoir excitation. With these two new measures of entanglement we can study in detail entanglement between the atom and the modes, and also between the modes.

In our analysis, we consider a Lorentzian reservoir and cover different dynamic regimes. For strong coupling we observe the periodic collapses and revivals of entanglement between the atom and the reservoir, which are associated with Rabi oscillations of the atom. Eventually, all the population leaves the atom and the reservoir becomes entangled. More precisely, two bundles of modes are excited, forming a "Bell-like" state. The method developed here, in terms of entanglement distributions, can also be used when considering various types of structured reservoirs. For example, reservoirs with a density of modes characterized by a band gap [9, 17, 18] can be treated with this method.

The paper is organized as follows. In section 2 we introduce a measure of

entanglement, the global entanglement, and apply it to our system-reservoir states when the number of degrees of freedom is finite. In section 3 we introduce the density of entanglement for the limit of a bath with an infinite number of modes. This entanglement measure evolves according to our model system as introduced in section 4. In section 5 we present our key results for the density of entanglement and we conclude in section 6.

2. Measures of multi-partite entanglement

Identifying and measuring entanglement in multi-partite systems presents various complications. Apart from the case of a two-qubit system, where entanglement can be identified both for a pure and a mixed state [19,20], multi-qubit entanglement is an open problem and to date several measures of entanglement have been proposed [1,2,21–24]. For the analysis that follows we will be using the global entanglement [23] since this will enable us to deal with many modes (or qubits). The physical problem we consider is that of entanglement between an atom and a reservoir, and in the context of this problem we will also consider the entanglement between different reservoir modes. To quantify this we will take a discrete bath of reservoir modes. Since we will assume only a single excitation in each bath mode, we can treat the bath states as a set of qubits for the purpose of computing the entanglement, and then later take a continuum limit. With just one excitation in total in the system, this excitation may be in the atom, or in the bath, so that the state vector at all times will have the form

$$|\psi(t)\rangle = c_0|\mathbf{0}\rangle + c_a(t)|\psi_a\rangle + \sum_\lambda c_\lambda(t)|\psi_\lambda\rangle, \tag{1}$$

where $|\mathbf{0}\rangle$ is the vacuum state

$$|\mathbf{0}\rangle = |0\rangle_a \otimes |0000\cdots000\rangle. \tag{2}$$

The other two states $|\psi_a\rangle$ and $|\psi_\lambda\rangle$, correspond to the atom being excited

$$|\psi_a\rangle = |1\rangle_a \otimes |000\cdots000\rangle, \tag{3}$$

or the mode λ of the reservoir being excited

$$|\psi_\lambda\rangle = |0\rangle_a \otimes |000\cdots01_\lambda0\cdots000\rangle. \tag{4}$$

Recently this kind of approach has been utilized for the study of decoherence and entanglement decay in systems with one or two excitations (effectively at $T = 0$) [25–56]. Some of this work examines the decay of a single excitation in a reservoir made from a continuum of modes [29–31, 42, 52] and other works examine entaglement with two or more qubits, but most still utilize the decay of a single excitation as considered in the present paper [25–28, 32–41, 43–46, 48, 50, 51].

If we started with a system of N qubits in a pure state $|\psi\rangle$, the global entanglement is defined as

$$Q(|\psi\rangle) = 2 - \frac{2}{N}\sum_{i=1}^{N} \mathrm{tr}\rho_i^2, \tag{5}$$

where ρ_i is the reduced density matrix for the i-th qubit. When $|\psi\rangle$ is a pure product state then $Q(|\psi\rangle) = 0$. If we take an entangled state for $|\psi\rangle$, such as the GHZ state

$$|GHZ\rangle_N = (|000\cdots\rangle + |111\cdots\rangle)/\sqrt{2}, \tag{6}$$

then $\mathrm{Q}(|\psi\rangle) = 1$. This example gives a maximum value for the global entanglement which is normalized such that $0 \leq Q(|\psi\rangle) \leq 1$. Another, more relevant example is the W-state

$$|W\rangle_N = \sum_{j=1}^{N} |0\cdots 01_j 0\cdots 0\rangle/\sqrt{N}, \tag{7}$$

for which the global entanglement goes to zero as $1/N$ for large N

$$\mathrm{Q}(|\psi\rangle) = 4(N-1)/N^2. \tag{8}$$

An important property of the global entanglement is that it is equal to a sum over two-qubit concurrences [2]. More specifically, for pure states $|\psi(t)\rangle$ [Equation (1)] we find from Equation (5), see the appendix for details, that

$$Q(|\psi\rangle) = \frac{2}{N+1} C^2(t), \tag{9}$$

where $C^2(t)$ reads

$$C^2(t) = \sum_{\lambda=1}^{N} c^2(\rho_{a\lambda}) + \sum_{1\leq\lambda<\mu\leq N} c^2(\rho_{\lambda\mu}). \tag{10}$$

The concurrence $c^2(\rho_{a\lambda})$ is that for the two-qubit (reduced) density matrix $\rho_{a\lambda}$ [19, 20]

$$\rho_{a\lambda} = \mathrm{tr}_{\mu\neq\lambda} \{|\psi(t)\rangle\langle\psi(t)|\} \tag{11}$$

between the atom and the λ-mode. The quantity $\rho_{\mu\lambda}$ is the corresponding density matrix for the modes μ and λ:

$$\rho_{\mu\lambda} = \mathrm{tr}_{a,\kappa\neq\lambda,\mu} \{|\psi(t)\rangle\langle\psi(t)|\}. \tag{12}$$

The two-qubit concurrence $c(\rho)$ is equal to [19, 20]

$$c(\rho) = \max\{0, \sqrt{\lambda_1} - \sqrt{\lambda_2} - \sqrt{\lambda_3} - \sqrt{\lambda_4}\}, \tag{13}$$

where λ_j are the eigenvalues of the matrix

$$R = \rho(\sigma_y \otimes \sigma_y)\rho^*(\sigma_y \otimes \sigma_y), \tag{14}$$

in decreasing order, i.e. $\lambda_1 > \lambda_2 > \lambda_3 > \lambda_4$, and σ_y is the relevant Pauli matrix.

Is is important to note here that $C^2(t)$ is exactly equal to the square of the norm of the concurrence vector [24], which is one of the many proposed measures for multi-partite entanglement. Because of the connection between $C^2(t)$ and the two-qubit concurrence Equation (10), we shall refer to $C^2(t)$ simply as the concurrence.

For the remainder of this work we will focus only on $C^2(t)$ and its properties since, with the exception of the normalization factor $2/(N+1)$ in Equation (9), it is equivalent to the global entanglement. Furthermore, we will be considering a continuum of reservoir modes, i.e. $N \gg 1$. In this limit, as we see in the following section, one can define a density of entanglement for continuous systems.

3. Density of entanglement

In the limit of continuous distribution for the reservoir modes, the summations in Equation (10) can be converted into integrals over the density of modes ρ_λ, i.e.

$$\sum_\lambda \to \int \mathrm{d}\omega_\lambda \rho_\lambda. \tag{15}$$

If we take this limit, the concurrence $C^2(t)$ can be expressed as the sum of two separate parts which ultimately involve either atomic population or reservoir mode populations:

$$C^2(t) = \int_{-\infty}^{\infty} d\omega_\lambda \mathcal{E}_A(\omega_\lambda, t) + \int_{-\infty}^{\infty} d\omega_\lambda \int_{-\infty}^{\infty} d\omega_\mu \mathcal{E}_R(\omega_\lambda, \omega_\mu, t). \tag{16}$$

The two distributions $\mathcal{E}_A$ and $\mathcal{E}_R$ will form the entanglement densities and are defined in terms of the two qubit concurrences to be

$$\mathcal{E}_A(\omega_\lambda, t) = c^2(\rho_{a\lambda})\rho(\omega_\lambda), \tag{17}$$

and

$$\mathcal{E}_R(\omega_\lambda, \omega_\mu, t) = \frac{1}{2} c^2(\rho_{\lambda\mu})\rho(\omega_\lambda)\rho(\omega_\mu), \tag{18}$$

where $\rho(\omega)$ is the reservoir density of modes. The interpretation for these two functions is now very simple.

The distribution $\mathcal{E}_A(\omega_\lambda, t)$ is the density of entanglement between the atom and all reservoir modes in the vicinity of mode ω_λ i.e. $\mathcal{E}_A(\omega_\lambda, t)\mathrm{d}\omega_\lambda$ is the total entanglement between the atom and all modes in the frequency interval ω_λ and $\omega_\lambda + \mathrm{d}\omega_\lambda$. In the same way $\mathcal{E}_R(\omega_\lambda, \omega_\mu, t)\mathrm{d}\omega_\mu$ gives the entanglement between the mode ω_λ and modes in the frequency range ω_μ to $\omega_\mu + \mathrm{d}\omega_\mu$.

For the remainder of this work, $\mathcal{E}_A$ will be referred as the atom-mode density of entanglement and to $\mathcal{E}_R$ as the mode-mode density of entanglement. The global entanglement $Q(|\psi\rangle)$, Equation (9), can be calculated from these two densities of entanglement, and thus a number of entanglement properties can be studied in terms of these two distributions. To this end it is important to note an interesting property for the two distributions $\mathcal{E}_A$ and $\mathcal{E}_R$. One can show that both entanglement distributions can be written in terms of the spectrum of reservoir excitation [57]

$$S(\omega_\lambda, t) = \rho(\omega_\lambda)|c_\lambda(t)|^2, \tag{19}$$

as

$$\mathcal{E}_A(\omega_\lambda, t) = 4|c_a(t)|^2 S(\omega_\lambda, t), \tag{20}$$

and

$$\mathcal{E}_R(\omega_\lambda, \omega_\mu, t) = 2S(\omega_\lambda, t)S(\omega_\mu, t)\,. \tag{21}$$

Thus, both entanglement distributions can be derived from the reservoir excitation spectrum. Having the definition for the entanglement density we can now introduce a Hamiltonian and dynamics to consider the time-dependent properties of entanglement for an atom coupled to a Lorentzian reservoir.

4. Dynamical model

The model system consists of a two-level atom coupled to a reservoir of harmonic oscillators with annihilation and creation operators a_λ and $a_\lambda^\dagger$ respectively. Within the rotating wave approximation the Hamiltonian reads ($\hbar = 1$)

$$H = \sum_\lambda \omega_\lambda a_\lambda^\dagger a_\lambda + \omega_0 |1\rangle_{aa}\langle 1| + \sum_\lambda g_\lambda \left(a_\lambda^\dagger |0\rangle_{aa}\langle 1| + a_\lambda |1\rangle_{aa}\langle 0| \right), \tag{22}$$

where g_λ is the coupling between the mode λ and the atomic transition $|1\rangle_a \rightarrow |0\rangle_a$. The atomic transition frequency is ω_0 whereas the λ-mode frequency is ω_λ. This model will preserve the assumption of a single excitation which is built into the system states in Equation (1).

For the purposes of the analysis that follows, it is very useful to introduce the reservoir structure function $D(\omega_\lambda)$ which reflects the properties of the density of modes [17]. This is defined through

$$\rho_\lambda (g_\lambda)^2 = \frac{\Omega_0^2}{2\pi} D(\omega_\lambda), \tag{23}$$

and is normalized such that

$$\int_{-\infty}^{\infty} \mathrm{d}\omega D(\omega) = 2\pi. \tag{24}$$

With this normalization a measure of the overall coupling strength is Ω_0 which is given by

$$\Omega_0^2 = \sum_\lambda (g_\lambda)^2. \tag{25}$$

Utilizing these assumptions, and a state vector of the form given by Equation (1), the Schrödinger equation in an interaction picture yields

$$\mathrm{i}\frac{\mathrm{d}}{\mathrm{d}t}\tilde{c}_a = \sum_\lambda g_\lambda e^{-\mathrm{i}\delta_\lambda t}\tilde{c}_\lambda, \tag{26}$$

$$\mathrm{i}\frac{\mathrm{d}}{\mathrm{d}t}\tilde{c}_\lambda = g_\lambda e^{\mathrm{i}\delta_\lambda t}\tilde{c}_a, \tag{27}$$

with the detuning between the atomic transition and the mode λ being given by

$$\delta_\lambda = \omega_\lambda - \omega_0. \tag{28}$$

The interaction picture amplitudes $\tilde{c}_a$ and $\tilde{c}_\lambda$ are connected to c_a and c_λ via a time-dependent transformation

$$\tilde{c}_a(t) = e^{\mathrm{i}\omega_0 t} c_a(t), \quad \tilde{c}_\lambda(t) = e^{\mathrm{i}\omega_\lambda t} c_\lambda(t). \tag{29}$$

Apart from numerical integration of equations (26) and (27), one could use analytical methods to derive the dynamics. Examples of these are: the resolvent method [9], the Laplace transform [58, 59] and that of the pseudomodes [17, 18, 42, 60]. This latter method applies when the spectral function is analytic with poles in the lower complex plane. Then equations (26) and (27) can be replaced, in the continuum limit,

by a set of equivalent equations where the atom now couples to a finite set of fictitious modes. Each of these modes has a one–to–one correspondence to the poles of $D(\omega)$.

For concreteness we consider Lorentzian reservoir structure functions of width Γ and peak frequency ω_c, i.e.

$$D(\omega) = \frac{\Gamma}{(\omega - \omega_c)^2 + (\Gamma/2)^2}. \tag{30}$$

This reservoir function has a simple pole at

$$z = \omega_c - \mathrm{i}\Gamma/2, \tag{31}$$

and for this $D(\omega)$ equations (26) and (27) are equivalent to two new equations

$$\mathrm{i}\frac{\mathrm{d}}{\mathrm{d}t}\tilde{c}_a(t) = \Omega_0\tilde{b}(t), \tag{32}$$

$$\mathrm{i}\frac{\mathrm{d}}{\mathrm{d}t}\tilde{b}(t) \ = (\Delta - \mathrm{i}\Gamma/2)\tilde{b}(t) + \Omega_0\tilde{c}_a(t), \tag{33}$$

where the atom-cavity detuning $\Delta = \omega_c - \omega_0$, and $b(t) = e^{-\mathrm{i}\omega_0 t}\tilde{b}(t)$ is the pseudomode amplitude. This set of equations can be associated with a master equation, where the physical interpretation for the pseudomode is that of a leaking cavity mode coupled to the atomic transition [17].

These coupled ODEs are straightforward to solve, and in particular, for the case of resonance, $\omega_c = \omega_0$, one finds for the atomic amplitude $c_a(t)$:

$$\tilde{c}_a(t) = \tilde{c}_a(0)e^{-\frac{\Gamma t}{4}}\left(\cosh(\alpha t/4) + \frac{\Gamma}{\alpha}\sinh(\alpha t/4)\right). \tag{34}$$

The modified decay rate α is given by

$$\alpha = \sqrt{\Gamma^2 - (4\Omega_0)^2} \tag{35}$$

in terms of Γ and Ω_0. For strong couplings, $4\Omega_0/\Gamma \gg 1$, the atomic population oscillates between the atom and the reservoir with a slowly decaying amplitude. In the long time limit all the energy is lost to the reservoir. If we decrease the coupling Ω_0, the atom dissipates its energy faster, and for $4\Omega_0/\Gamma \ll 1$ the atom exponentially decays into the reservoir. These two types of behavior are illustrated in Figure 1 which is given as a reference point for the entanglement discussion in the next section. The figures show the atomic population for $\Omega_0 = 10\Gamma$ and $\Omega_0 = 0.1\Gamma$ plotted against time t.

5. Evolution of reservoir entanglement

5.1. Entanglement generation by decay

The interaction between the atom and the reservoir results in entanglement creation between the atom and the reservoir modes, and also between the reservoir modes. This latter entanglement is indirect and is due to the effective coupling between the modes as a result of their interaction with the atom. When considering our measure of the total entanglement, the concurrence $C^2(t)$ as a function of time (Figure 2), we see that for both strong and weak coupling the concurrence builds up to a maximum value equal

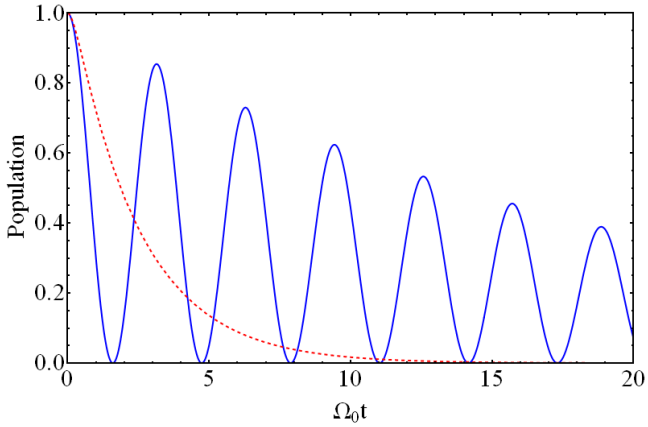

Figure 1. The atomic population $|c_a(t)|^2$ as a function of time for strong coupling $\Omega_0 = 10\Gamma$ (solid line), and weak coupling $\Omega_0 = 0.1\Gamma$ (dashed line). Both results were obtained from Equation (34). The initial system state in this and the following figures is defined by $c_a(0) = 1$, $c_0 = 0$ and all $c_\lambda(0) = 0$. The detuning $\Delta = 0$.

to $C^2(t) = 2$. In the case of strong coupling, Figure 2(a), the concurrence reaches the maximum value very quickly, and then oscillates in a way which is closely connected to the Rabi oscillations seen in Figure 1. The oscillations return to the maximum value of two, with a minimum value that also approaches two as time increases. If we compare the concurrence to the population in Figure 1 we see that every minimum in concurrence is matched by a peak in population of the atomic state. Likewise the maxima in concurrence are matched by minima in the atomic population: it seems that the decaying atom is very efficient at generating entanglement in the reservoir. At this point we note that at long times the energy has left the atom (see the population Figure 1) and the system is in an approximate product state of unexcited atom and bath states. The large value of the concurrence at these times indicates the presence of entanglement in the bath. In the long time limit the concurrence reaches a steady value $C^2(\infty) = 2$, a result that can be derived analytically if one uses Eqs. (16) (20) and (21) and the spectrum for $t \to \infty$. This limit for the concurrence is the same in the weak coupling case, see Figure 2(b); the atom decays exponentially and the entanglement reaches a steady state monotonically. In the long time limit the atom again disentangles from the reservoir and entanglement is distributed only between the reservoir modes.

By examining the entanglement densities [Eqs. (17,18)] we can gain further insight into where the entanglement resides in this system and how it evolves over time. In Figure 3 we show the atom-bath density of entanglement $\mathcal{E}_A(\omega_\lambda, t)$ for both strong and weak couplings. The strong coupling case shows a complex behavior. First a central peak of entanglement appears in the vicinity of $\omega_\lambda \approx \omega_0$; note the peak at $\delta_\lambda \approx 0$ for short times in Figure 3(a). The entanglement is then transferred to Rabi sidebands at $\delta_\lambda = \delta_\pm \approx \pm\Omega_0$. The sideband entanglement oscillations seen take place at half the

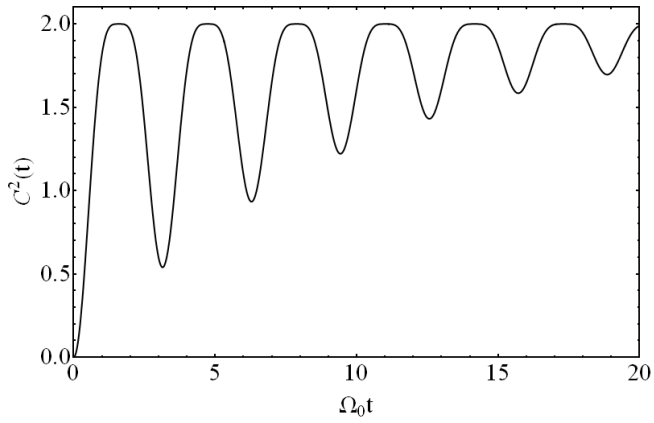

(a)

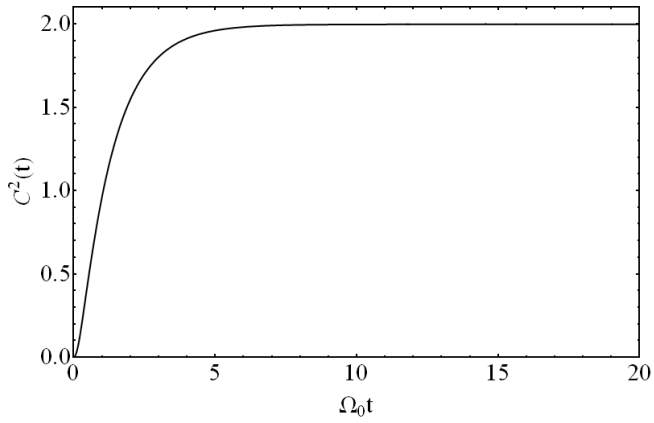

(b)

Figure 2. The concurrence $C^2(t)$ as a function of time for different couplings $\Omega_0 = 10\Gamma$ (a) and $\Omega_0 = 0.1\Gamma$ (b). The result was obtained from Eqs. (16), (20) and (21).

frequency of the central peak entanglement oscillations. Ultimately all the entanglement decays at long times, $\mathcal{E}_A(\omega_\lambda, t) \to 0$, as there can be no entanglement between bath and atom when the atomic population approaches zero. At that point the entanglement indicated by the concurrence in Figure 2(a) must reside in reservoir mode entanglement which is examined in the next section, Sec. 5.2. Figure 3(a) shows that as Rabi sidebands develop in the reservoir excitation, the atom-bath entanglement moves from central frequencies to the sidebands at $\delta_\lambda = \delta_\pm$. The period doubling of the central peak is due to the oscillations of the excitation there, combined with the oscillations of atomic population. The population of the sideband modes is more stable, but oscillations of the atomic population result in oscillations of entanglement there, too.

For weak coupling, Figure 3(b), the entanglement briefly resides across the whole reservoir structure. This is essentially because the coupling of the atom is over this same range. In weak coupling, however, Rabi sidebands do not develop. Instead the final

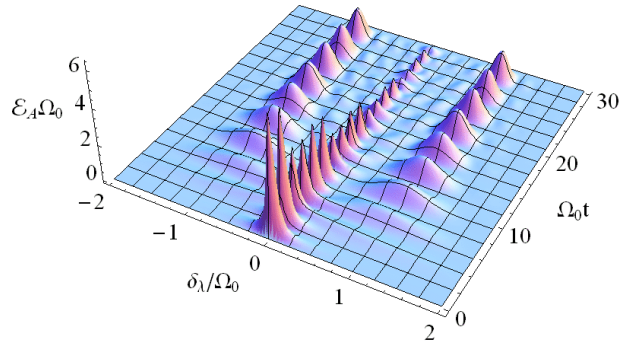

(a)

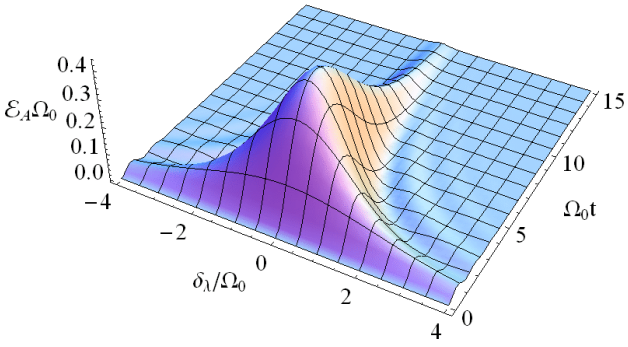

(b)

Figure 3. The density of entanglement $\mathcal{E}_A(\omega_\lambda, t)$ between atom and bath is plotted for different times t and reservoir mode frequencies ω_λ. The coupling strength is: (a) $\Omega_0 = 10\Gamma$; and (b) $\Omega_0 = 0.1\Gamma$.

population of bath modes will be over a relatively narrow frequency range well within the model Lorentzian profile, Equation (30). Since both atomic, and mode population is needed for atom-bath entanglement, the narrow central frequency region is entangled only for a short while and then decays.

5.2. Entanglement between reservoir modes

As already mentioned, coupling the atom and the reservoir modes will induce an indirect coupling between the reservoir modes. Because of this, the modes will entangle and it is important to consider the properties of the mode-mode density of entanglement $\mathcal{E}_R$. In the long time limit one can easily obtain analytic expressions for the spectrum of excitation in the reservoir and from that calculate the density of entanglement for $t \to \infty$. Using the definition for the spectrum of reservoir excitation Equation (19))

with the solution 34 and Equation (27), we find that for $t = \infty$

$$S(\omega_\lambda, \infty) = \frac{\Omega_0^2 D(\omega_\lambda)}{2\pi} \cdot \frac{\delta_\lambda^2 + (\Gamma/2)^2}{(\delta_\lambda^2 - \Omega_0^2)^2 + (\Gamma/2)^2\delta_\lambda^2}, \\ = \frac{\Omega_0^2 \Gamma/2}{\pi[(\delta_\lambda^2 - \Omega_0^2)^2 + (\Gamma/2)^2\delta_\lambda^2]}, \tag{36}$$

where, as before, $\delta_\lambda = \omega_\lambda - \omega_0$ [Equation (28)]. Taking Equation (36) together with Equation (21) it is straightforward to calculate the mode-mode density of entanglement for $t \to \infty$

$$\mathcal{E}_R(\omega_\lambda, \omega_\mu, \infty) = \frac{\Omega_0^4 \Gamma^2}{2\pi^2 \left[(\delta_\lambda^2 - \Omega_0^2)^2 + (\Gamma/2)^2\delta_\lambda^2\right] \left[(\delta_\mu^2 - \Omega_0^2)^2 + (\Gamma/2)^2\delta_\mu^2\right]}. \tag{37}$$

Figure 4 shows the mode-mode density of entanglement for several couplings and in the limit $t \to \infty$. In the strong coupling case, Figure 4(a), we see the formation of four sharp peaks which signify the existence of strong entanglement between the two symmetric modes $\delta_\pm$ as a result of the Rabi splitting. This picture has a simple and rather intuitive interpretation: the final state for the reservoir has the form of a Bell-like state between the two symmetric modes $\delta_\pm \approx \pm\Omega_0$. First we note that the final state takes the approximate form

$$|\psi(\infty)\rangle = |0\rangle_a \otimes \sum_{\lambda=1}^{N} \left(P_+(\omega_\lambda) + P_-(\omega_\lambda)\right) |\psi_\lambda\rangle. \tag{38}$$

where the two probability distributions $|P_\pm(\omega_\lambda)|^2$ are centered at $\delta_\lambda = \delta_+$ and δ_- respectively. For $\Omega_0 \gg \Gamma$, i.e. in the strong coupling regime, their width is very small which practically means that only the two modes $\delta_\pm$ are excited and, for this, the reservoir state can be approximately described by a Bell state of the form

$$|\psi(\infty)\rangle \approx |0\rangle_a \otimes |0_{\omega \neq \omega_0 + \delta_\pm}\rangle \otimes \left(|1_+ 0_-\rangle + e^{\mathrm{i}\phi}|0_+ 1_-\rangle\right)/\sqrt{2}, \tag{39}$$

where ϕ is an arbitrary phase factor. This picture applies only at long times. For short times the mode-mode density of entanglement will initially have a distribution that peaks in the vicinity of $\omega_\lambda \approx \omega_\mu \approx \omega_0$. As time evolves this distribution breaks into four symmetrical peaks seen in Figure 4(a), as a result of the Rabi splitting.

For moderate and weaker couplings, $\Omega_0 = \Gamma$ and $\Omega_0 \ll \Gamma$, the simple patterns observed in Figure 4(a) for the mode-mode density of entanglement due to the Rabi splitting disappear. For example in Figure 4(b) the density of entanglement for $t \to \infty$ and $\Omega_0 = \Gamma$ is plotted. From this we can see that, for moderate couplings, although the distribution peaks around $\delta_\mu = \delta_\lambda = \delta_\pm$, the entanglement spreads over a wider range of reservoir frequencies. For even weaker couplings, Figure 4(c), only modes in the vicinity of $\omega_\lambda \approx \omega_0$ are excited and thus the entanglement is created only between modes in this frequency range. This is the reason for having a peaked entanglement distribution with a centre at $\omega_\mu = \omega_\lambda = \omega_0$.

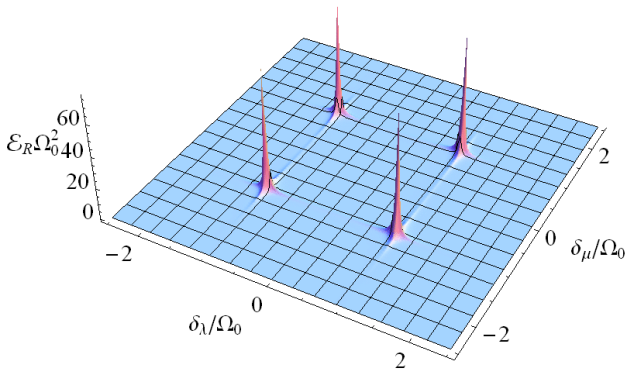

(a)

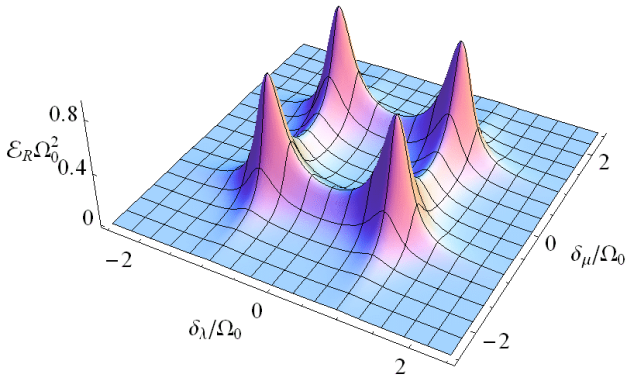

(b)

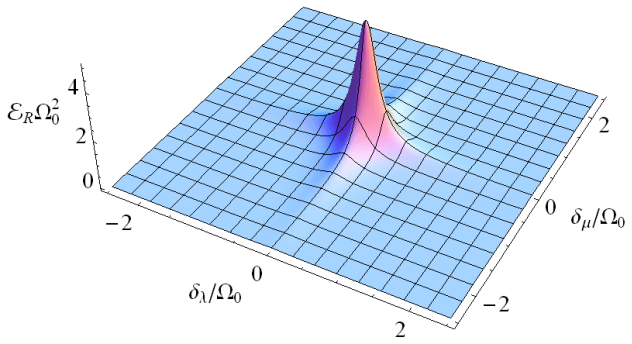

(c)

Figure 4. The density of entanglement $\mathcal{E}_R(\omega_\lambda, \omega_\mu, t)$ between bath modes for $t \to \infty$. The coupling strength is: (a) $\Omega_0 = 10\Gamma$; (b) $\Omega_0 = \Gamma$; and (c) $\Omega_0 = 0.1\Gamma$.

6. Conclusion

In this work we have presented a method for studying entanglement between a two-level atom and a large reservoir of modes such as may be found in, for example, a lossy cavity field. Our aim was to study entanglement between the atom and the reservoir, and within the reservoir itself. To do this we restricted our interest to a simple case where the reservoir modes can be treated as qubits. Using global entanglement, we derived the entanglement densities $\mathcal{E}_A$ and $\mathcal{E}_R$ for the reservoir modes. These distributions have been given in terms of the well known two-qubit concurrences, and can be calculated from the reservoir excitation spectrum. The entanglement densities are then used both for studying entanglement between the atom and the reservoir modes, and also between the modes.

In considering different dynamical regimes defined in terms of the coupling strength, we noticed that when strong interactions occur, the reservoir modes are entangled in a "Bell-like" state in the long time limit. This long time limit is a regime where no excitation remains in the atom and all the entanglement is amongst the reservoir modes. Since there is no direct interaction between the bath-modes, see the Hamiltonian 22, the final entanglement arises through indirect interaction. Another way of viewing this is that in the strong coupling regime we have a non-Markovian system. In such a case, as the atom decays, some information resides in part of the reservoir in a way that it can be returned to the atom later [34]. This allows the indirect coupling between the reservoir modes which creates the entanglement. In the weak coupling (Markovian) case, the information does not return to the atomic system and the reservoir entanglement cannot be created.

In the transition from strong to weak coupling, the "Bell-like" state of Figure 4(a) coalesces into a single peaked structure as was seen in Figure 4(c). Based on the interpretation given above we would expect that the transition to a single peak takes place as the system becomes Markovian rather than non-Markovian. In principle this could be tested with a measure of non-Markovianity [61].

In conclusion, when considering entanglement between an atom and a large reservoir, the analysis can be formulated in terms of entanglement density functions. These distributions can be associated with the spectrum of reservoir excitation, a quantity that can be measured, for example, in cavity QED experiments. Although the model considered here, an atom coupled to a Lorentzian reservoir, is rather simple, it can be extended to consider more complicated reservoir structures such as model photonic band gaps. Potentially, one could consider generalizations for the density of entanglement, and also extend the model beyond the assumption of a single excitation in the system.

Acknowledgments

This work has been supported in part by the European Commission's ITN project FASTQUAST. S.M. acknowledges financial support from the Turku Collegium of Science and Medicine, The Emil Aaltonen foundation and the Finnish Cultural Foundation. J.P. acknowledges financial support from the Magnus Ehrnrooth Foundation and the Academy of Finland (project 133682).

Appendix A. Global entanglement

For the completeness of our analysis, we show here how the global entanglement for the pure state $|\psi(t)\rangle$, Equation (1), can be derived. First, the state $|\psi(t)\rangle$ can be written as a pure state of $N+1$ qubits, i.e.

$$|\psi(t)\rangle = c_0|\mathbf{0}\rangle + \sum_j c_j(t)|\psi_j\rangle, \tag{A.1}$$

where $j = a$ for the atom, or $j = \lambda = 1, \cdots, N$ for the reservoir modes. The vacuum state $|\mathbf{0}\rangle$ is given in Equation (2), while $|\psi_j\rangle = |\psi_a\rangle$ [Equation (3)] for $j = a$, or is given by Equation (4) if $j = \lambda$, i.e. refers to a reservoir mode.

Next we calculate the reduced two-qubit density matrix ρ_{ji}

$$\rho_{ji} = \mathrm{tr}_{k\neq j,i}\{\rho\} = \langle\chi_0|\rho|\chi_0\rangle + \sum_{k\neq j,i}\langle\chi_k|\rho|\chi_k\rangle, \tag{A.2}$$

where $|\chi_0\rangle$ is the $N-2$-qubit vacuum state

$$|\chi_0\rangle = \prod_{k\neq i,j}|0_k\rangle, \tag{A.3}$$

and $|\chi_k\rangle$ is the $N-2$-qubit state with a single excitation, i.e.

$$|\chi_k\rangle = |0\cdots 01_k 0\cdots 0\rangle. \tag{A.4}$$

With these definitions for $|\chi_0\rangle$ and $|\chi_k\rangle$, the reduced density matrix takes the form

$$\rho_{ji} = \begin{pmatrix} 1-|c_j|^2-|c_i|^2 & c_0^*c_i & c_0^*c_j & 0 \\ c_0c_i^* & |c_i|^2 & c_jc_i^* & 0 \\ c_0c_j^* & c_j^*c_i & |c_j|^2 & 0 \\ 0 & 0 & 0 & 0 \end{pmatrix}, \tag{A.5}$$

where the basis states, starting from top and moving to bottom, are

$$|0_j0_i\rangle, \quad |0_j1_i\rangle, \quad |1_j0_i\rangle, \quad |1_j1_i\rangle. \tag{A.6}$$

The concurrence $c(\rho_{ji})$, Equation (13), for this density matrix reads

$$c^2(\rho_{ji}) = 4|c_j|^2|c_i|^2. \tag{A.7}$$

In order to calculate the global entanglement, we derive the single qubit density matrix from Equation (A.5) by tracing out the i-qubit

$$\rho_j = \begin{pmatrix} 1-|c_j|^2 & c_0c_j^* \\ c_0^*c_j & |c_j|^2 \end{pmatrix}, \tag{A.8}$$

where the basis states are $|0_j\rangle$ and $|1_j\rangle$. Using this we first calculate ρ_j^2 and then its trace

$$\mathrm{tr}\rho_j^2 = 1 + 2|c_j|^2\left(|c_j|^2 + |c_0|^2 - 1\right), \tag{A.9}$$

which after using probability conservation becomes

$$\mathrm{tr}\rho_j^2 = 1 - 2|c_j|^2 \sum_{i\neq j} |c_i|^2. \tag{A.10}$$

Substituting in Equation (5) for the global entanglement we have

$$Q(|\psi\rangle) = \frac{2}{N+1} \sum_j \sum_{i\neq j} 2|c_j|^2|c_i|^2. \tag{A.11}$$

Separating the atom-mode terms and the mode-mode terms, and taking into account the symmetry of the two-qubit concurrence

$$c^2(\rho_{ji}) = c^2(\rho_{ij}), \tag{A.12}$$

it takes the form

$$Q(|\psi\rangle) = \frac{2}{N+1}\left(\sum_{\lambda=1}^{N} c^2(\rho_{a\lambda}) + \sum_{1\leq\lambda<\mu\leq N} c^2(\rho_{\lambda\mu})\right), \tag{A.13}$$

which leads to the result of Eqs. (9) and (10).

References

[1] Amico L, Fazio R, Osterloh A and Vedral V 2008 *Rev. Mod. Phys.* **80** 517
[2] Horodecki R, Horodecki P, Horodecki M and Horodecki K 2009 *Rev. Mod. Phys.* **81** 865
[3] Nielsen M A and Chuang I L 2000 *Quantum computation and quantum information* (Cambridge: Cambridge University Press)
[4] Leibfried D, Blatt R, Monroe C and Wineland D 2003 *Rev. Mod. Phys.* **75** 281–324
[5] Dalfovo F, Giorgini S, Pitaevskii L P and Stringari S 1999 *Rev. Mod. Phys.* **71** 463–512
[6] Leggett A J 2001 *Rev. Mod. Phys.* **73** 307–356
[7] Raimond J M, Brune M and Haroche S 2001 *Rev. Mod. Phys.* **73** 565–582
[8] Varcoe B T H, Brattke S and Walther H 2004 *New J. Phys.* **6** 97
[9] Lambropoulos P, Nikolopoulos G M, Nielsen T R and Bay S 2000 *Rep. Prog. Phys.* **63** 455–503
[10] Nikolopoulos G M, Lambropoulos P and Proukakis N P 2003 *J. Phys. B: At. Mol. Opt. Phys.* **36** 2797–2816
[11] Lazarou C, Nikolopoulos G M and Lambropoulos P 2007 *J. Phys. B: At. Mol. Opt. Phys.* **40** 2511–2529
[12] Nikolopoulos G M, Lazarou C and Lambropoulos P 2008 *J. Phys. B: At. Mol. Opt. Phys.* **41** 025301
[13] Cummings N I and Hu B L 2008 *Phys. Rev. A* **77** 053823
[14] Leandro J and Semio F 2009 *Opt. Comm.* **282** 4736 – 4740
[15] Haroche S and Raimond J M 2006 *Exploring the quantum* (New York: Oxford University Press)
[16] Breuer H P and Petruccione F 2002 *The theory of open quantum systems* (New York: Oxford University Press)
[17] Garraway B M 1997 *Phys. Rev. A* **55** 2290–2303
[18] Garraway B M 1997 *Phys. Rev. A* **55** 4636–4639
[19] Hill S and Wootters W K 1997 *Phys. Rev. Lett.* **78** 5022–5025

[20] Wootters W K 1998 *Phys. Rev. Lett.* **80** 2245–2248
[21] Mintert F, Carvalho A R, Kus M and Buchleitner A 2005 *Phys. Rep.* **415** 207–259
[22] Barnum H, Knill E, Ortiz G, Somma R and Viola L 2004 *Phys. Rev. Lett.* **92** 107902
[23] Meyer D A and Wallach N R 2002 *J. Math. Phys.* **43** 4273–4278
[24] Akhtarshenas S J 2005 *J. Phys. A: Math. Gen.* **38** 6777–6784
[25] Bellomo B, Lo Franco R and Compagno G 2007 *Phys. Rev. Lett.* **99** 160502
[26] Bellomo B, Lo Franco R, Maniscalco S and Compagno G 2008 *Phys. Rev. A* **78** 060302
[27] Maniscalco S, Francica F, Zaffino R L, Lo Gullo N and Plastina F 2008 *Phys. Rev. Lett.* **100** 090503
[28] Wang F Q, Zhang Z M and Liang R S 2008 *Phys. Rev. A* **78** 042320
[29] Frishman E and Shapiro M 1996 *Phys. Rev. A* **54** 3310–3321
[30] Fussell D P and Dignam M M 2008 *Phys. Rev. A* **77** 053805
[31] Thanopulos I, Brumer P and Shapiro M 2008 *J. Chem. Phys.* **129** 194104
[32] Al-Amri M, Li G x, Tan R and Zubairy M S 2009 *Phys. Rev. A* **80** 022314
[33] Li Y, Zhou J and Guo H 2009 *Phys. Rev. A* **79** 012309
[34] Mazzola L, Maniscalco S, Piilo J, Suominen K A and Garraway B M 2009 *Phys. Rev. A* **80** 012104
[35] Mazzola L, Maniscalco S, Piilo J and Suominen K A 2010 *J. Phys. B: At., Mol. Opt. Phys.* **43** 085505
[36] Zhou J, Wu C, Zhu M and Guo H 2009 *J. Phys. B: At. Mol. Optic. Phys.* **42** 215505
[37] Ferraro E, Scala M, Migliore R and Napoli A 2009 *Phys. Rev. A* **80** 042112
[38] Francica F, Maniscalco S, Piilo J, Plastina F and Suominen K A 2009 *Phys. Rev. A* **79** 032310
[39] Xiao X, Fang M F, Li Y L, Zeng K and Wu C 2009 *J. Phys. B: At. Mol. Opt. Phys.* **42** 235502
[40] Zhang Y J, Man Z X and Xia Y J 2009 *Eur. Phys. J. D* **55** 173–179
[41] Mazzola L, Maniscalco S, Suominen K and Garraway B 2009 *Quantum Inf. Process.* **8** 577–585
[42] Mazzola L, Maniscalco S, Piilo J, Suominen K A and Garraway B M 2009 *Phys. Rev. A* **79** 042302
[43] He Z, Zou J, Shao B and Kong S Y 2010 *J. Phys. B: At. Mol. Opt. Phys.* **43** 115503
[44] Zhang Y J, Man Z X, Zou X B, Xia Y J and Guo G C 2010 *J. Phys. B: At. Mol. Opt. Phys.* **43** 045502
[45] Man Z X, Zhang Y J, Su F and Xia Y J 2010 *Eur. Phys. J. D* **58** 147–151
[46] Man Z X, Zhang Y J, Su F and Xia Y J 2010 *Eur. Phys. J. D* **58** 147–151
[47] Zhang Y J, Man Z X, Xia Y J and Guo G C 2010 *Eur. Phys. J. D* **58** 397401
[48] Tong Q J, An J H, Luo H G and Oh C H 2010 *Phys. Rev. A* **81** 052330
[49] Mazzola L, Bellomo B, Lo Franco R and Compagno G 2010 *Phys. Rev. A* **81** 052116
[50] Tong Q J, An J H, Luo H G and Oh C H 2010 *Phys. Rev. A* **81** 052330
[51] Wang B, Xu Z Y, Chen Z Q and Feng M 2010 *Phys. Rev. A* **81** 014101
[52] Tong Q J, An J H, Luo H G and Oh C H 2010 *J. Phys. B: At. Mol. Opt. Phys.* **43** 155501
[53] Fanchini F F, Werlang T, Brasil C A, Arruda L G E and Caldeira A O 2010 *Phys. Rev. A* **81** 052107
[54] Hamadou-Ibrahim A, Plastino A R and Zander C 2010 *J. Phys. A: Math. Theor.* **43** 055305
[55] Li J G, Zou J and Shao B 2010 *Phys. Rev. A* **81** 062124
[56] Xu Z Y, Yang W L and Feng M 2010 *Phys. Rev. A* **81** 044105
[57] Linington I E and Garraway B M 2006 *J. Phys. B: At. Mol. Opt. Phys.* **39** 3383–3401
[58] John S and Quang T 1994 *Phys. Rev. A* **50** 1764–1769
[59] Kofman A G, Kurizki G and Sherman B 1994 *J. Mod. Opt.* **41** 353–384
[60] Dalton B J, Barnett S M and Garraway B M 2001 *Phys. Rev. A* **64** 053813
[61] Breuer H P, Laine E M and Piilo J 2009 *Phys. Rev. Lett.* **103** 210401